Vol. 11, No. 3, 2025

Ihor Kuzio¹, Nadiia Maherus², Yurii Sholoviy³

Department of Robotics and Integrated Mechanical Engineering Technologies, Lviv Polytechnic National University, 12, S. Bandery str., Lviv, Ukraine, E-mail: ihor.v.kuzo@lpnu.ua, ORCID 0000-0001-9271-6505
 Department of Robotics and Integrated Mechanical Engineering Technologies, Lviv Polytechnic National University, 12, S. Bandery str., Lviv, Ukraine, E-mail: nadiia.i.maherus@lpnu.ua, ORCID 0000-0003-1946-8503
 Department of Robotics and Integrated Mechanical Engineering Technologies, Lviv Polytechnic National University, 12, S. Bandery str., Lviv, Ukraine, E-mail: yurii.p.sholovii@lpnu.ua, ORCID 0000-0003-0154-7983

IMPROVING DRIVE SYSTEM EFFICIENCY FOR LARGE-SCALE ROTARY KILNS

Received: September 02, 2025 / Revised: September 16, 2025 / Accepted: October 06, 2025

© Kuzio I., Maherus N., Sholoviy Yu., 2025

https://doi.org/10.23939/ujmems2025.03.086

Abstract. The objective of the present article is to ascertain the forces emanating from the interface between the girth gear and the pinion, which exert a direct influence on both the loading of the kiln supports and the selection of an optimal open-gear drive configuration for large-scale rotary units. Significance. Ensuring the straightness of the kiln shell axis constitutes a pivotal challenge in the design and operation of large rotary units. Deviations, even those measuring a mere millimeter, in long, heavily loaded kilns have been shown to redistribute support reactions, increase shell bending, raise radial loads in bearing assemblies, and induce noise and vibration. These phenomena, in turn, have been demonstrated to accelerate wear and increase the risk of failure. Mitigation of these adverse factors necessitates a thorough examination of gear-mesh loading to ensure stable, full-face tooth contact, as well as design solutions that are impervious to installation and assembly inaccuracies. This approach is a simple yet effective means of enhancing the reliability and service life of open-gear drives and their associated drive systems. **Methodology.** The study examined the loads generated in the gear contact zone and investigated how the geometric arrangement of the drive elements affected these loads. **Results.** The proposed mathematical relationships facilitate the evaluation of forces within the gear mesh, thereby establishing the dependence of mesh parameters on the geometric arrangement of the lever-mounted pinion. **Scientific novelty.** Mathematical relationships have been developed to quantify the influence of gear-mesh parameters and the geometric positioning of rotary-kiln open-gear drive elements on contact zone loads and their transmission to the support assemblies. The practical significance of the aforementioned topic is as follows: The paper presents an efficient open-gear drive configuration for a large-scale unit, providing calculation results to support the selection of appropriate geometric parameters, thereby ensuring effective operation.

Keywords: rotary kilns, girth gear, pinion, intermediate gear, open-gear drive, support reaction force, large-scale unit, mesh parameters.

Introduction

In recent years, the industry has placed growing emphasis on assuring the quality, reliability, and service life of large-scale process equipment. This trend is driven by stricter requirements for uninterrupted production, rising energy costs, and the need to reduce operating expenses throughout the entire machine life cycle. These challenges are particularly pronounced for rotary cement kilns, whose stable operation directly governs both throughput and product quality.

The operation of rotary kilns combines high-temperature processes with substantial mechanical loading of the primary load-carrying members (shell, support rollers, and drive). Prolonged thermal exposure, shell ovalization and deflection, installation errors, and component wear redistribute support reactions, raise contact stresses in tribological interfaces and gear meshes, and increase vibration and noise levels. The consequences are accelerated wear, unplanned downtime, higher specific energy consumption, and elevated failure risk, all of which directly degrade reliability and durability metrics.

Within cement manufacturing, the kiln is the keystone of the process line, affecting the chemical transformation of the raw mix into clinker through successive stages of preheating, decarbonation, and sintering. Accordingly, stringent requirements are imposed on its design, installation accuracy, lubrication quality, and operating conditions. The selection and justification of the drive, supports, and thermal-regime parameters must be based on validated engineering models and the results of in-situ measurements.

Review of Modern Information Sources on the Subject of the Paper

The selection and application of kiln drives is an evolving field. Typical drive configurations for cement kilns, motor types, and an overview of their operating regimes for efficient kiln operation are reviewed in [1]. The market also offers various advanced technologies related to kiln speed control and drive modernization. Currently, the most prevalent drive types for cement kilns include open-gear drives, which utilize a girth gear and pinion, friction-roller drives, and hydraulic and hydrostatic drives [1–3]. In large cement kilns, open-gear solutions with a girth gear and pinion remain the standard for most installations; modern equipment designs often employ dual-pinion drives to achieve high power ratings [1]. The continuing popularity of open-gear drives stems from several advantages: the ability to deliver high torque, critical for maintaining stability in large equipment; slip-free starting during run-up; simplicity of design; high maintainability; and compatibility with various motor technologies.

One of the primary challenges in designing and operating large rotating equipment is maintaining the straightness of the shell axis. Even millimeter-scale deviations in long, heavy kilns can redistribute loads, causing the support reactions and wear of bearing assemblies to increase sharply, thereby raising the risk of failure. Axis misalignment induces elevated loads on the supports, shell bending, increased loading of bearing units, and higher noise and vibration levels. Numerous studies have addressed the analysis and diagnostic methods for axis straightness deviations, as well as recommendations for their mitigation [4–7]. Analyses of permissible tolerances, manufacturing and installation errors, together with theoretical results, indicate that these requirements cannot always be met in practice; actual deviations may exceed existing limits by a factor of approximately 2–6 [8]. Moreover, several studies analyze the loading within the contact zone of drive components using computational simulations. These investigations are typically performed on individual industrial units and do not enable a parametric assessment of how the geometry of specific drive elements influences the loading [9, 10]. It is therefore expected that all these factors affect the performance of the open-gear drive of the rotating unit, thereby significantly reducing its reliability.

Research methods

The operational performance of large-scale unit drives is governed by the contact loading within the gear mesh, since the magnitude and direction of the mesh forces directly determine the loads transmitted to the supports. Accordingly, analytical models were formulated for an open-gear drive with a lever-mounted pinion: without an intermediate gear and with an intermediate gear. Equilibrium equations were derived for the tangential, radial, and axial components of the mesh force and expressed as functions of the geometric arrangement of the drive elements.

Therefore, this study aimed to investigate how gear-mesh geometry affects the loads generated during operation.

Research results

One of the simplest yet most effective open-gear arrangements for rotary kiln drives is the lever-mounted pinion configuration (Fig. 1). In this configuration, the pinion (1) is mounted on a lever (2) whose pivot axis (3) lies along the gear-mesh line of action – that is, along the direction of the resultant R of the

Ihor Kuzio, Nadiia Maherus, Yurii Sholoviy

tangential F_{τ} and radial F_{τ} mesh-force components. This geometry aligns the resultant mesh force R with the lever pivot, thereby minimizing the contact normal force required to press the pinion (1) against the girth gear (4) even in the presence of installation errors and small center-distance offsets. The pressing force is provided by a spring pack (5) with adjustable preload; as a result, the pinion follows the girth gear, compensating shifts of the kiln rotation axis during operation. An essential element of this drive configuration is the use of self-aligning supports [3], which furnish angular and radial compliance without introducing secondary bending moments.

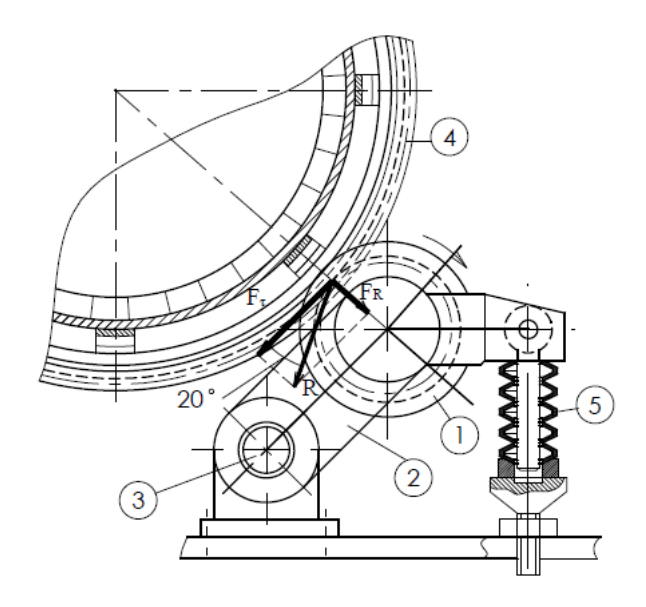


Fig. 1. Drive configuration with a lever-mounted pinion gear

From a force-transfer standpoint, the advantage of the lever-mounted pinion design is that the lever and the drive frame carry the resultant mesh force; the elastic element supplies only the minimal biasing force and acts as a damper of micro-vibrations rather than a primary load-carrying member. This yields several benefits:

- reduced sensitivity of the gear set to installation errors (radial and partially compensates for angular);
 - stabilized contact pattern over the tooth face width and lower local contact stresses;
 - decreased vibration levels and impact loads during tooth engagement;
 - improved lubrication in the open-gear pair owing to a more uniform pressure distribution.

Structurally, the assembly requires appropriate selection of spring-pack stiffness and lever travel, as well as a suitable preload-adjustment range. In practice, it is essential to provide:

- travel stops and damping inserts to attenuate peak load impulses;
- reliable targeting of the lubricant jet at the tooth-entry zone;
- monitoring of backlash and alignment as the kiln shell heats (shell ovality and deflection).

At the same time, this configuration has notable limitations. The most significant is the deterioration of operating conditions for the intermediate shaft connecting the pinion to the gearbox output. As a consequence, the shaft is subjected to elevated bending stresses and variable bearing loads. This may necessitate a larger shaft diameter, stiffer bearing supports, or the use of flexible/self-aligning couplings, and the assembly remains sensitive to angular misalignment. Another drawback is that, when the spatial position of the gears changes in service, the meshing teeth have limited capacity for self-alignment across the face width; as a result, edge loading and accelerated wear may occur.

To mitigate these shortcomings, an improved drive configuration with an intermediate gear can be employed (Fig. 2). The drive configuration (Fig. 2) incorporates an intermediate gear (1), which receives torque from the gearbox output shaft. In this configuration, the displacement of the pinion (2) with its lever

does not affect the operation of the intermediate connections. However, the service life of the pinion teeth is reduced because of simultaneous engagement with two gears (1) and (3).

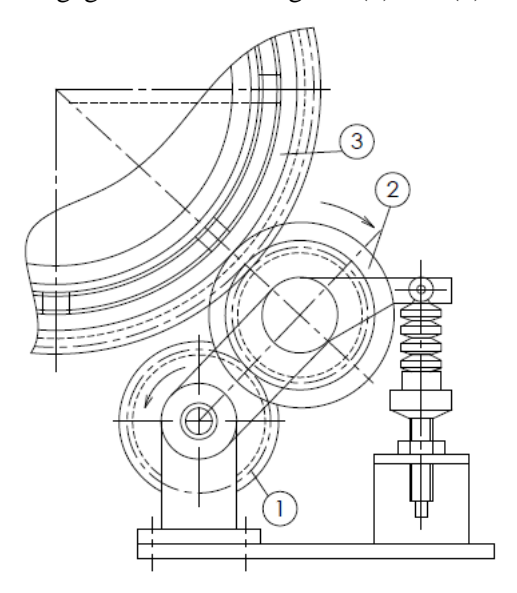


Fig. 2. Drive configuration with a lever-mounted pinion and an intermediate gear

Inserting an intermediate gear between the gearbox output shaft and the pinion allows one to:

- reduce bending loads and secondary bending moments on the intermediate shaft;
- provide additional degrees of freedom for tooth self-alignment radially (via the lever) and partially across the face width (via self-aligning supports of the intermediate gear and appropriate couplings/floating bearings);
 - tune the biasing force more precisely.

This modernization, however, requires careful engineering trade-offs, as the increased gear-mesh count raises total frictional losses and noise, the lubrication and sealing system becomes more complex, and stricter manufacturing tolerances and maintenance regimes are demanded. Accordingly, when choosing between the basic lever configuration (Fig. 1) and the improved one with an intermediate gear (Fig. 2), a comparative assessment should be performed against criteria such as bearing and shaft life, tooth contact-fatigue strength, vibroacoustic performance, energy consumption, and maintainability.

For the drives under consideration, it is advisable to perform a force analysis of the gear-mesh elements. In the most widely used drive configuration today, the pinion meshes directly with the girth gear and is mounted on a fixed pivot O_1 (Fig. 3). The mesh forces in this case are determined by the relations given below.

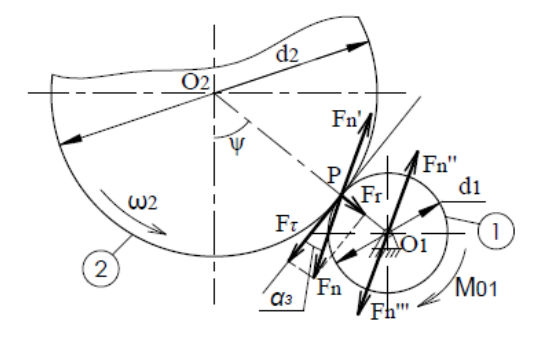


Fig. 3. Free-body diagram of the widely used drive

The normal (line-of-action) force is given by:

$$F_n = \frac{M_{01}}{d_1 \cdot \cos(\alpha_3)},\tag{1}$$

where M_{01} is the torque referred to the pinion axis of rotation; d_1 is the pinion pitch diameter; α_3 is the pressure angle.

The tangential (circumferential) force at the gear mesh can be determined from the following equation:

$$F_{\tau} = F_n \cdot \cos(\alpha_3). \tag{2}$$

The radial (separating) force at the gear mesh is given by the equation:

$$F_r = F_\tau \cdot \tan(\alpha_3). \tag{3}$$

At the pivot O_1 , a force acts whose magnitude equals F_n , while its direction depends on the angle ψ . For the design shown in Fig. 1, several configurations are possible in general. In the first configuration, pivot A of lever 3 lies on the line of action, as shown in Fig. 4.

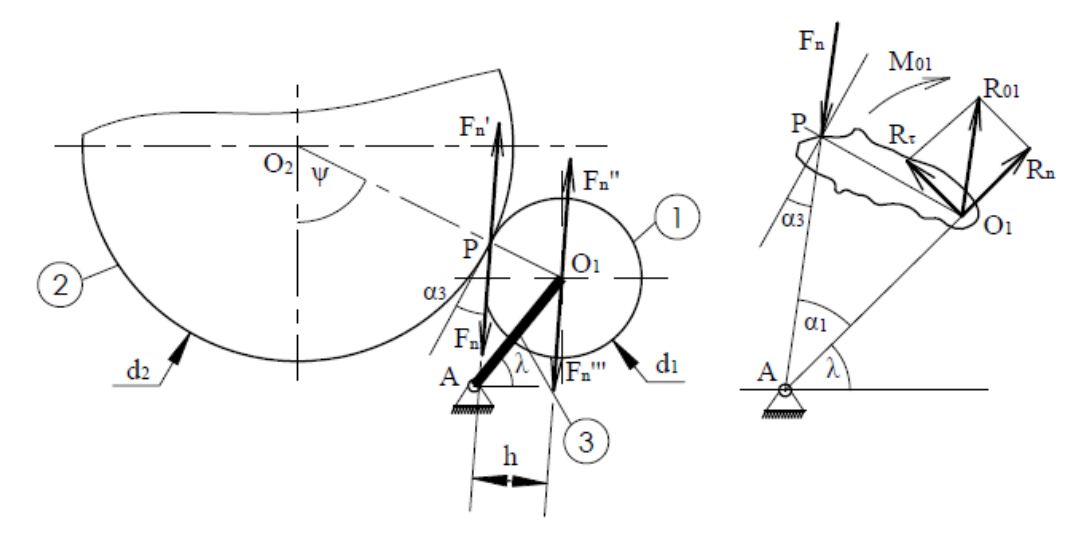


Fig. 4. Free-body diagram of the lever-mounted pinion – girth gear mesh

Considering the lever AO_1 (Fig. 4), the normal and tangential components of the reaction at the pivot O_1 can be determined as follows:

$$R_n = F_n(\cos(\alpha_1 + \lambda)\cos\lambda + \sin(\alpha_1 + \lambda)\sin\lambda), \tag{4}$$

$$R_{\tau} = F_{\tau}(\sin(\alpha_1 + \lambda)\cos\lambda - \cos(\alpha_1 + \lambda)\sin\lambda),\tag{5}$$

where α_1 is the angle between the direction of the normal force F_n and the lever AO_1 ; λ is the inclination of the lever AO_1 relative to the horizontal ($\alpha_1 + \lambda = 90^\circ$).

The resultant reaction at the pivot O_1 is given by:

$$R_{01} = \sqrt{R_{\tau}^2 + R_n^2} = F_n. \tag{6}$$

The resultant reaction R_{01} is parallel to the direction of the normal force F_n , since:

$$\tan(\varphi) = \frac{R_n}{R_n} = \tan(\alpha_1). \tag{7}$$

The force acting on the link AO_1 is opposite in direction to the reaction R_{01} and does not pass through the point A. Consequently, a moment F_nh arises that tends to rotate the link AO_1 clockwise about A. To keep the link in equilibrium at the required position, a counteracting moment must be applied, which can be provided by an additional spring device (Fig. 1).

Another case occurs when the point A lies on a line parallel to the line of action and passing through the pinion center, the couple formed by F_n and F_n'' balances the torque M_{01} (Fig. 5). The force F_n'' is directed along the link AO_1 . For a standard involute mesh with the pressure angle $\alpha_3 = 20^\circ$, if $\psi = 70^\circ$, then the force F_n is vertical; consequently, there is no force tending to displace the pivot A.

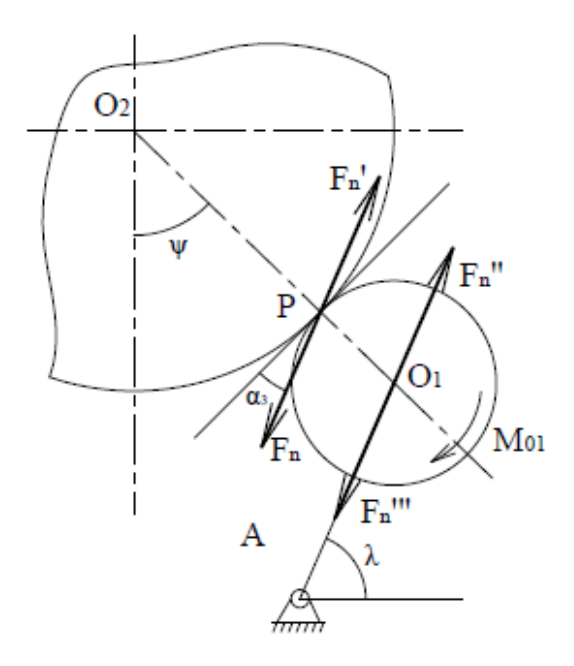


Fig. 5. Free-body diagram of the gear mesh with the lever aligned parallel to the line of action

During operation, gear teeth wear and the pressure angle may vary. Consequently, the line of action of the force F_n''' can deviate from the vertical, creating a moment about the point A. To ensure proper rolling contact of the gears (i.e., minimal slip), a dedicated spring-loaded biasing device should be employed.

When the intermediate gear is incorporated into the drive (Fig. 2), the force distribution becomes more involved (Fig. 6). At the intermediate gear, two equal normal forces F_n and F_n' act at the mesh contact points P_1 and P_2 ; their vector sum yields a resultant whose magnitude and direction depend on the position of the lever-mounted pinion relative to the intermediate gear.

By applying the law of sines to the geometry in Fig. 6, the following relations are obtained:

$$\frac{r_1 + r_n}{\sin(\varphi)} = \frac{r_1 + r_2 + \Delta g}{\sin(\beta)},\tag{8}$$

$$r_2 + r_n = (r_1 + r_2 + \Delta g)\cos(\varphi) + (r_1 + r_n)\cos(\beta),$$
 (9)

where r_1 is the pinion pitch radius; r_n is the intermediate gear pitch radius; r_2 is the girth gear pitch radius; Δg is the distance between the girth gear and the pinion; φ , β are angles defined by the relative arrangement of the gears in mesh (Fig. 6).

Using Eq. (9), the angle φ is given by:

$$\cos(\varphi) = \frac{r_2 + r_n}{2(r_1 + r_n)} + \frac{r_1 + r_n}{2(r_2 + r_n)} - \frac{(r_1 + r_2 + \Delta g)^2}{2(r_2 + r_n)(r_1 + r_n)}.$$
(10)

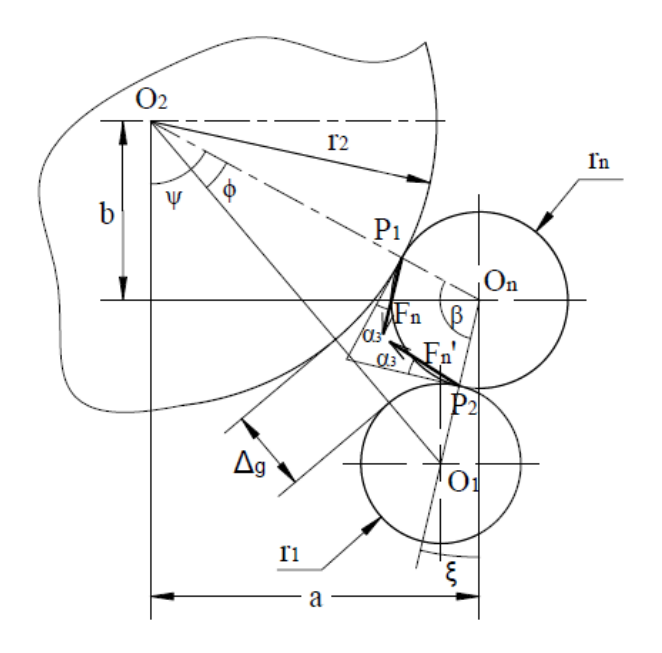


Fig. 6. Free-body diagram of a three-gear train (intermediate gear – lever-mounted pinion – girth gear)

The distance Δg must satisfy the following limits:

$$2m + f \le \Delta g \le 2r_n,\tag{11}$$

m is the gear module; f is the distance between the addendum circles of the pinion and the girth gear. The distance Δg can be determined from the following equation:

$$\Delta g = \sqrt{(b + (r_1 + r_n)\cos(\xi))^2 + (a - (r_1 + r_n)\sin(\xi))} - (r_1 + r_2). \tag{12}$$

where $a = (r_2 + r_n)\sin(\psi)$; $b = (r_2 + r_n)\cos(\psi)$.

Thus, the distance Δg can be expressed in terms of the numbers of teeth z_1, z_2, z_n of the pinion, girth gear, and intermediate gear, respectively:

$$\Delta g = 0.5m \left(\sqrt{(z_1 + z_n)^2 + (z_2 + z_n)^2 - 2(z_1 + z_n)(z_2 + z_n)\cos(\beta)} - (z_1 - z_2) \right).$$
 (13)

From Eq. (13), the angle β can be determined as

$$\beta = \operatorname{acos}\left(\frac{z_1 + z_2}{2(z_2 + z_n)} + \frac{z_2 + z_n}{2(z_1 + z_n)} - \frac{z_1 + z_2 + 2\Delta g/m}{2(z_1 + z_2)(z_2 + z_n)}\right). \tag{14}$$
Consequently, the number of teeth on the intermediate gear z_n is:

$$z_n = \frac{\sqrt{z_1 + z_2} - (z_1 + z_2)}{2} + \frac{1}{m} \sqrt{\frac{2\Delta g + 2m\Delta g(z_1 + z_2) + m^2 z_1 z_2 (1 + \cos(\beta))}{1 - \cos(\beta)}}.$$
 (15)

Analysis of the last expression leads to the following conclusions. For the resultant force to vanish R=0, the intermediate gear must have at least $z_n=101$ and the angle $\beta=40^\circ$ (the calculation uses parameters of the existing rotary kiln drive 5x185m, namely $z_1 = 20$, $z_2 = 150$ i m = 45 mm). Such an intermediate gear can not be accommodated in the design, as its overall dimensions would be comparable to those of the girth gear. Therefore, the intermediate gear must have fewer teeth; in that case, the resultant force is nonzero and is given by:

$$R = n_a * F_n, \tag{16}$$

where $n_g = \sqrt{2(1 + cos(\theta_g))}$; θ_g is the angle between the forces F_n and F_n' .

The angle between the forces F_n and F_n must then satisfy the limit:

$$\theta_a = 220^\circ - \beta. \tag{17}$$

The coefficient n_g relates the resultant force R to normal force F_n and enables assessment of the influence of drive configuration features, namely, the distance between the pinion and the girth gear Δg , on n_g (Fig. 7). As the diagram (Fig. 7) indicates, the resultant force R, which tends to pull the intermediate gear toward the girth gear, decreases markedly with increasing overall dimensions. It is advisable to locate the pinion below the line O_2O_n , and the distance Δg should be kept to a minimum.

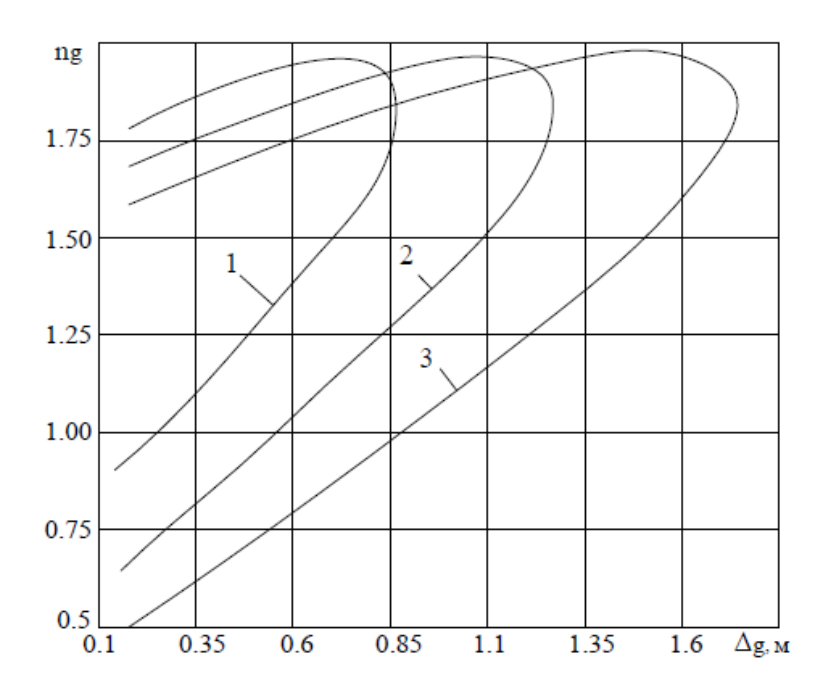


Fig. 7. Variation of the coefficient n_g with the distance Δg : 1) $-z_n = 20$; 2) $-z_n = 30$; 3) $-z_n = 40$

Conclusions

A comprehensive examination of the key force factors that directly influence both tooth contact and the loads at the support points was conducted. This examination was based on a thorough analysis of force interactions in the gear mesh of open drives for large industrial units. The paper puts forth a series of effective design configurations for this particular class of equipment. The beneficial effect of incorporating an intermediate gear in the drive is demonstrated. An analysis of the variation of the coefficient with distance for different intermediate gear sizes indicates that the limiting distance between the girth gear and the pinion varies with tooth count. The ratio of the resultant force to the normal force is contingent on two variables: the intermediate gear size and the distance.

References

- [1] G. Seggewiss, N. Schachter, and G. Obermeyer, "Kiln Drive Application Considerations", in 2005 IEEE-IAS/PCA Cement Industry Technical Conference, Kansas City, 2005, pp. 52–76.
- [2] J. A. Standen, "Installation of a Hydraulic Kiln Drive to Eliminate a Resonant Vibration Problem", in *1996 IEEE/PCA Cement Industry Technical Conference*, Los Angeles, 1996, pp. 35–43.
- [3] K. A. Geiger, B. P. Keefe, G. R. Kotz, and R. E. Freiherr von Kaernten, "The friction drive for modern two-support kilns", in 2004 IEEE-IAS/PCA Cement Industry Technical Conference, Chattanooga, 2004.

Ihor Kuzio, Nadiia Maherus, Yurii Sholoviy

- [4] K. Zheng, Y. Zhang, L. Liu, and C. Zhao, "An online straightness deviation measurement method of rotary kiln cylinder", *Tehnicki vjesnik (Technical Gazette)*, vol. 24, No. 5, pp. 1297–1305, 2017.
- [5] Ľ. Kovanič, P. Blistan et al., "Analytical Determination of Geometric Parameters of the Rotary Kiln by Novel Approach of TLS Point Cloud Segmentation," *Applied Sciences*, vol. 10, No. 21, p. 7652, 2020.
- [6] Y. Xiao, X. Li, and X. Chen, "General solution to kiln support reactions and multi-objective fuzzy optimization of kiln axis alignment", *Structural and Multidisciplinary Optimization*, vol. 36, pp. 319–327, 2008.
- [7] Y. Shen, S. Wang, X. Li, and B. S. Dhillon, "Multiaxial fatigue life prediction of kiln roller under axis line deflection", *Applied Mathematics and Mechanics*, vol. 31, pp. 205–214, 2010.
- [8] A. O. Kychma and R. Ya. Predko, "Loading of structural elements of large-sized rotating aggregates during long-term operation", *Academic Journal. Industrial Machine Building, Civil Engineering*, No. 1(50), pp. 25–35, 2018.
- [9] D. J. Van Dyk and L. Pretorius, "Analysis of dynamic effects in a rotary kiln system used for iron production", *R&D Journal*, vol. 11, No. 1, pp. 12–20, 1995.
- [10] A. Deshpande and A. Utpat, "Comparative Analysis for Bending and Contact Stresses of Girth Gear By Using AGMA Standard & Finite Element Analysis", *International Journal of Innovative Research in Science, Engineering and Technology (IJIRSET)*, vol. 3, No. 10, pp. 16946–16952, October, 2014.